The 2009 IEEE/RSJ International Conference on
Intelligent Robots and Systems
October 11-15, 2009 St. Louis, USA

Mechanical Modeling Characterization of Biological Cells Using Microrobotics Cell Injection Test Bed

Youhua Tan, Dong Sun, and Wenhao Huang

Abstract—**Mechanical properties of biological cells play an important role in regulating cellular functions. Some micromanipulation methods have been reported in the literature to measure cell mechanics, but they are either high-costly or difficultly-operated. This paper presents our approach to use microrobotic cell injection technology as the test bed to characterize the mechanical properties of biological cells, by virtue of low cost and easy operation. By extending our previous work [41], we develop a mechanical model to interpret the mechanical responses during microinjection and extract the cells properties. Both finite element analysis and microinjection experiments are performed to verify the mechanical model. It is shown that the results obtained from the proposed mechanical model agree well with that obtained from finite element analysis and the experiments. Elastic moduli of zebrafish embryos at different developmental stages are characterized. This demonstrates not only the validity of the proposed model but also the fact that the microrobotic cell injection technology combining with the mechanical model can be used to characterize the mechanical properties of biological cells.**

I. Introduction

Microinjection of biological cells using robotics device has received considerable attentions in recent years [1-4], due to its wide applications in intracytoplasmic sperm injection (ICSI), pro-nuclei DNA injection, gene therapy, to name a few. Increasing demands for both high precision and high throughput in cell manipulation highlights the need for automated processing with robotics technology. A good mechanical modeling of cells enables this automated process to succeed.

Mechanical properties of biological cells play an important role in regulating cellular functions. Many recent researches suggest that the cell mechanical properties may be used as a diagnostic indicator for the onset and progression of some diseases. For example, the transformed human chondrosarcoma cells with a decreasing malignancy show a decrease in cell modulus and viscosity [5]. Distinct Young's moduli are detected in prostate cancer cells with differing metastatic potential [6]. The metastatic cancer cells are much softer than their benign counterparts [7-10]. The average elastic constants of malignantly transformed fibroblasts are significantly lower than that of normal ones [11]. Red blood cells parasitized by plasmodium falciparum become rigid and poorly deformable, and show abnormal circulatory behavior [12]. Young's modulus of the virus shell in the mature form is fourfold higher than that of the immature form [13]. These researches suggest that the mechanical properties of cells may be regarded as an indicator to the pathogenesis of certain diseases.

With the great development of micromanipulation technology, many experimental techniques have emerged as reliable and effective tools in measuring the mechanical properties of biological cells, which include micropipette aspiration [14-15], atomic force microscopy [16-18], cell poker [19-20], micro-plate manipulation [21-22], magnetic tweezers [23], optical tweezers [24-26], and optical stretcher [27]. These techniques, however, are either high costly or difficult to be implemented.

Microinjection technology has been studied extensively and been proved to be an effective technique to introduce foreign materials into a biological cell [28-30]. Benefiting from the great advance, such as immobilization and recognition of biological cells [3, 31-32], autofocusing algorithms [33], visual servoing control [1], injection force sensing [2, 4, 34-39], and batch manipulation [2, 4, 40], some semi-automatic and fully-automatic microrobotic cell injection systems have been developed. With these microinjection systems, the injection force and the cell deformation can be well controlled. Nonetheless, few researches have been reported that microrobotic cell injection can be used to characterize the mechanical properties of biological cells. Here, due to the merits of low cost and easy operation, we demonstrate that microrobotic cell injection technology in combination with an appropriate modeling approach can be used to characterize the mechanical properties of biological cells.

Extending our previous work [41], in this paper, we utilize a microinjection mechanical model to interpret the cell mechanical responses during injection. Finite element analysis and cell injection experiments are performed to verify this model in prediction. Through the identification procedure, the elastic moduli of zebrafish embryos at different developmental stages are obtained. It is shown that the results both from the experiments and the finite element analysis agree well with that from the mechanical model, which demonstrates the fact that the microrobotic cell injection combining with a mechanical modeling methodology can be used to estimate mechanical

This work was supported by a grant from Research Grants Council of the Hong Kong Special Administrative Region, China [Reference No. CityU 120709], UGC Special Equipment Grant [SEG_CityU 01], and a grant from City University of Hong Kong [Reference No. 9360131].

Y. H. Tan is with the Control and Mechatronics Group, Suzhou Research Institute of City University of Hong Kong and University of Science and Technology of China, Suzhou, China (e-mail: tanyh@mail.ustc.edu.cn, tel: 86-512-87161281, fax: 86-512-87161381).

Dong Sun is with the Department of Manufacturing Engineering and Engineering Management, City University of Hong Kong, Kowloon, Hong Kong (e-mail: medsun@cityu.edu.hk).

W. H. Huang is with the Department of Precision Machinery and Precision Instrumentation, University of Science and Technology of China, Hefei, China (e-mail: whuang@ustc.edu.cn).

properties of biological cells.

II. Mechanical Modeling

A mechanical model [41] is developed to describe the interaction between an injector and a probed cell membrane. This model is based on membrane theory, and neglects the contribution of bending rigidity reasonably due to the small membrane thickness of biological cells [42-44]. Biomembrane is assumed to be an incompressible, homogeneous, and elastic continuum, which has been used in most of continuum modeling of cell membranes to make the complicated problem tractable [43-47]. In our proposed model, contact between the injector and the membrane is determined by two governing equations, which take the forms of

$$\frac{\partial T_1}{\partial \lambda_1}\lambda_1' + \frac{\partial T_1}{\partial \lambda_2}\lambda_2' = \frac{\rho'}{\rho}(T_2 - T_1) \quad (1)$$

$$K_1 T_1 + K_2 T_2 = P \quad (2)$$

where T_1 and T_2 are the principal tensions, λ_1 and λ_2 are the principal stretch ratios, K_1 and K_2 are the principal curvatures. The indices 1 and 2 refer to the corresponding component in the meridian and circumferential directions of the deformed membrane, respectively. P is the cell turgor pressure acting on the membrane, ρ is the transverse coordinate after deformation, and the prime denotes the derivative with respect to a specific angle ψ which is related to the cell deformation (see Fig. 1).

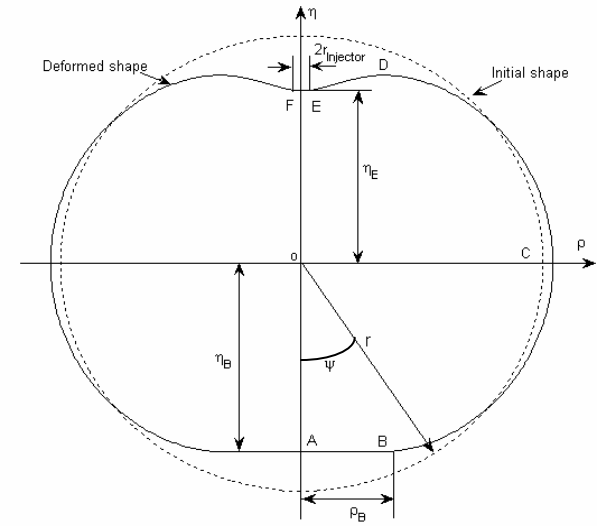

Fig. 1. Coordinates definition before and after microinjection.

In the mechanical model, the biomembrane is assumed to behave like a nonlinear Mooney-Rivlin material with the strain energy function denoted by W .

$$W = C_1(I_1 - 3) + C_2(I_2 - 3) = C_1[(I_1 - 3) + \alpha(I_2 - 3)] \quad (3)$$

where C_1 and C_2 are the material parameters with the dimension of stress and $\alpha = C_2 / C_1$. I_1 and I_2 are strain invariants, which can be expressed as functions of λ_1 and λ_2 [45]. For a homogeneous and isotropic, incompressible elastic material C_1 is equal to $\frac{E}{6(1+\alpha)}$ (E is elastic modulus).

The principal tensions T_i can be obtained as follows,

$$T_i = \frac{h}{\lambda_1 \lambda_2}\lambda_i \frac{\partial W(\lambda_1, \lambda_2)}{\partial \lambda_i}, \ (i = 1, 2) \quad (4)$$

where h is the membrane thickness.

After proper coordinate definitions, K_1 , K_2 and ρ can all be expressed as a function of λ_1 and λ_2 , respectively (see more details in [41]). Hence, the unknown quantities in the governing equations (1) and (2) are λ_1 , λ_2 and ψ . Given appropriate constraints and boundary conditions, the governing equations can be solved by a numerical algorithm, e.g., Runge-Kutta method [48]. The deformed cell shape can then be calculated, from which the cell deformation d is obtained. The indentation force F can be acquired based on the force balance. As a result, the relationship between the indentation force and the cell deformation is established.

$$F = P\pi\rho_B^2 = P\pi(r_0\lambda_{2B}\sin\psi_B)^2 \quad (5)$$

$$d = 2r_0 - (\eta_E - \eta_B) \quad (6)$$

where r_0 is the initial radius of biological cells.

Through the solution of the governing equations, it is found that different values of the material parameters lead to different force-deformation relationships, which ensures the uniqueness of the mechanical properties of biological cells.

III. Model Verification and Property Characterization

Both finite element (FE) analysis and microrobotic cell injection experiments are conducted to verify the mechanical model. After model verification, the mechanical properties of zebrafish embryos at different developmental stages are characterized.

A. Finite element analysis

The zebrafish embryos used in the experiments were assumed to be spherical before cell injection in the commercial FE software ANSYS (ANSYS 8.0, PA, USA), which was shown in Fig. 2. Since the imposed force and the geometry were symmetrical, half of the cell was analyzed. Considering that the injector and substrate were much stiffer than biological cells, they were thus represented as the upper and lower rigid half-cylinders, respectively. Hyperelastic material, e.g., Mooney-Rivlin material, was used to describe the deformation behavior of the biomembrane. The shell 41 incompressible membrane element was adopted to discretize the computational domain of the cell model. Since the contribution of the bending rigidity was neglected in the mechanical model, the deformation behavior of the shell 41 elements was set to just bear the tensional stress with no compliance to bending moment. The spacing ratio of the element size in the contact and noncontact regions was set to 1/6 to acquire the injection force with high accuracy at a relatively low computational cost.

The mesh density was carefully chosen to make sure that the solution process was converged and the accuracy of the analysis results was acceptable.

Appropriate constraints and boundary conditions must be applied to make sure the FE simulation was performed correctly. Since the volume of the biological cell was assumed to keep constant, the turgor pressure P should be regulated to meet this constraint at different deformations.

Given the material parameters, when the cell deformation was prescribed, the needed injection force could be calculated through the solution of the FE model, and vice versa. Therefore, if the hyperelastic material was assigned with various material parameters, a series of force-deformation curves would be obtained.

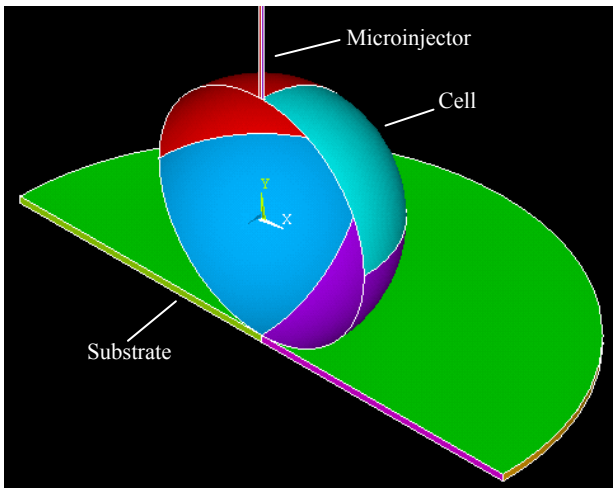

Fig. 2. The FE model for microinjection analysis.

B. *Microrobotic cell injection experiments*

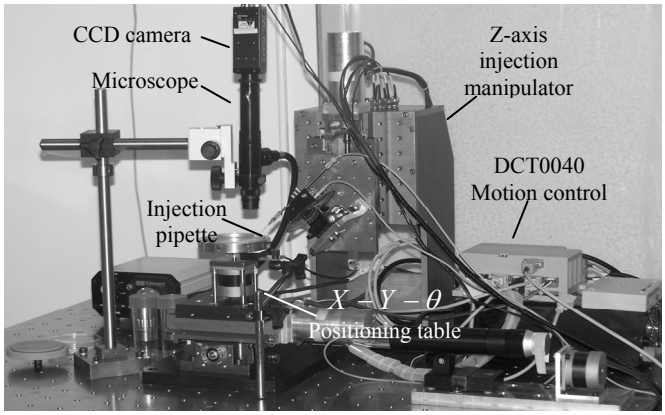

Fig. 3. Microrobotic cell injection system.

Fig.3 illustrates the experimental setup of our microrobotic cell injection system [37]. It mainly consists of three modules: an executive module, a sensory module, and a control module. The executive module includes a $X-Y-\theta$ positioning table and a Z-axis injection manipulator where an injection pipette is mounted. Biological cells are placed and immobilized on the working plate. The motion between the $X-Y-\theta$ table and the Z-axis manipulator is coordinated to perform cell injection task. The sensory module mainly contains a PVDF (polyvinylidene fluoride) micro force sensor, an optical microscope, a CCD camera, and a PCI image capture card. The control module consists of a host computer (PD 2.8GHz) and a DCT0040 motion control/drive system provided by DynaCity Technology (HK) Ltd [49]. All of the mechanical components were supported upon an anti-vibration table.

Zebrafish embryos with radii of 500 μm were selected as samples for the experiments. For force measurement experiments, 60 embryos were collected according to the standard procedures [50], where 20 at the blastula stage (3 hours post fertilization, abbr. 3hpf), 20 at the segmentation stage (12hpf), and 20 at the pharyngula stage (26hpf).

The detailed control strategy and injection process are described in [35-36]. Here, a brief description is given as follows. At the pre-piercing step, the contour of the embryo is obtained after appropriate image processing. The centroid is thus found, where the microinjector should be aligned. Then, the coordinated motion naturally makes sure that the microinjector tip points towards the center of the injected embryo. When the injector tip approaches the embryo, the velocity achieves the maximum. At the piercing step, the microinjector indents the biomembrane until the embryo is broken. The injector is driven in the opposite direction to be pulled out of the biomembrane at the post-piercing step. Fig. 4 illustrates this injection process.

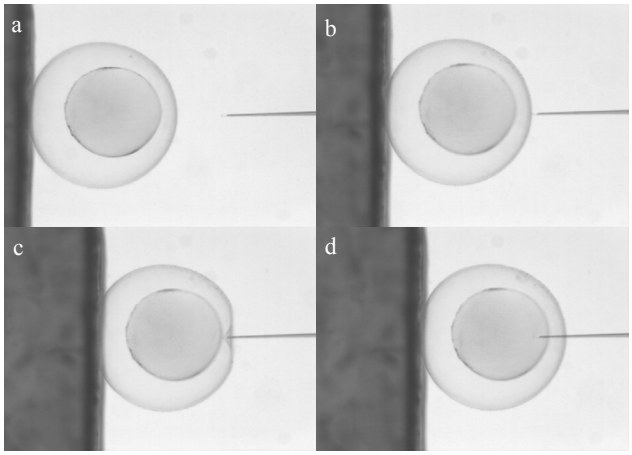

Fig. 4. Microinjection of zebrafish embryos: (a) at the pre-piercing step, (b) the injector tip approaching the embryo, (c) at the piecing step, (d) breakage of the biomembrane.

The PVDF force sensor is bound to the end of a microinjctor and utilized to measure the injection force in real time. The time when the injector contacts the cell is known as the instant when the measured injection force has a sudden rise. Although the CCD camera can detect the deformation of the injected cell with a frame rate of 60Hz, it needs some image processing procedures and has less position accuracy. In our experiment, the encoder information from the DC motor is sampled into the motion controller to calculate the position trajectory. With information of both the force and the position trajectory, the

relationship between the injection force and the deformation can be obtained during the microinjection process.

Zebrafish embryos at three developmental stages were used for microinjection. During all of the experiments, the same motion profile was adopted. Some typical injection forces are plotted in Fig. 5. It is shown that the injection forces overlap very well, which implies that microrobotic injection process is repeatable and reproducible and the mechanical properties of the injected embryos are similar. The repeatable microinjection experiments pave the way for effective acquirement of force-deformation relationships and for reliable measurement of cell mechanics.

The experimental force-deformation results are shown in Fig. 6. It is shown that the slopes of these curves are different at various developmental stages of zebrafish embryos. When a prescribed deformation is imposed, the needed injection force for the embryos at the blastula stage is the largest, whereas the least force is required for the embryos at the pharyngula stage, which indicates the softening of the embryos. Moreover, the relationship between the injection force and the cell deformation is nonlinear, especially at large deformation.

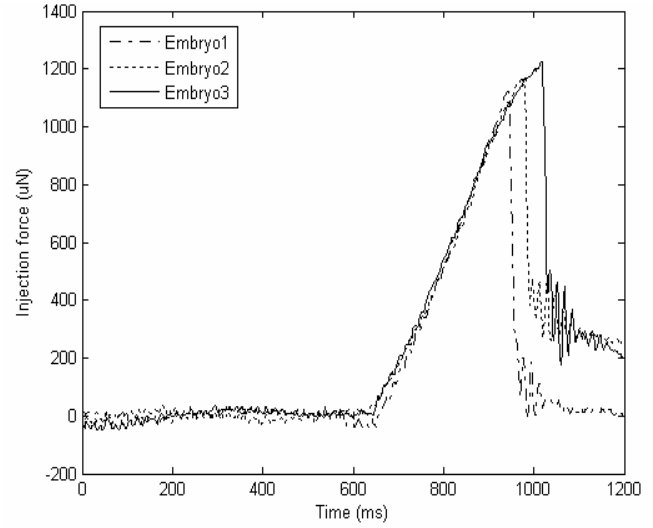

Fig. 5 Injection force of zebrafish embryos at the blastula stage.

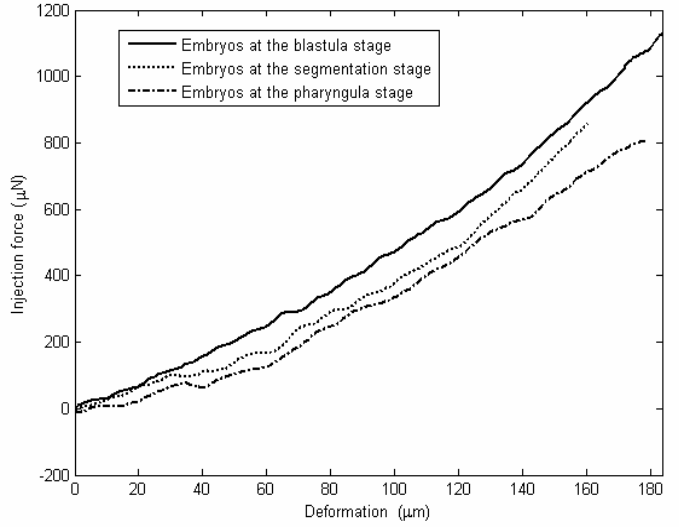

Fig. 6. Experimental results of zebrafish embryos at different developmental stages.

C. Identification of mechanical property

Due to lack of sufficient study, the material parameters in the strain energy function are manually adjusted. To match the numerical simulation to the experiments, the parameters must be chosen appropriately. In this paper, we follow the method of Schmidt et al. [51] by using a deviation parameter δ , which is a quantitative measure of the fitness between the mechanical modeling and the experimental data and defined as

$$\delta=\frac{1}{n}\sum_{i=1}^{n}\left[\frac{F_e(i)-F_s(i)}{F_e(i)}\right]^2 \tag{7}$$

where n is the number of the sampled experimental results, $F_e(i)$ is the ith experimental force value, and $F_s(i)$ is the corresponding modeling force. When the material parameters are prescribed, the value of δ can be calculated. The best fitness will be realized when δ is minimized, and then the mechanical properties of biological cells can be identified.

D. Model verification and property characterization

The FE analysis results of zebrafish embryos at different developmental stages are shown in Fig.7. It is shown that the difference of the results obtained from FE analysis and from the mechanical model is very small, which demonstrates our developed model is in concert with the FE simulation. It is worth noting that FE results become more accurate with finer meshed elements, which will complicate the iteration calculation and increase the computational cost. A compromise should be made between the computational const and accuracy. Moreover, both of the results indicate the nonlinear relationship between the injection force and the induced cell deformation, which may result from both of the geometry nonlinearity and material nonlinearity.

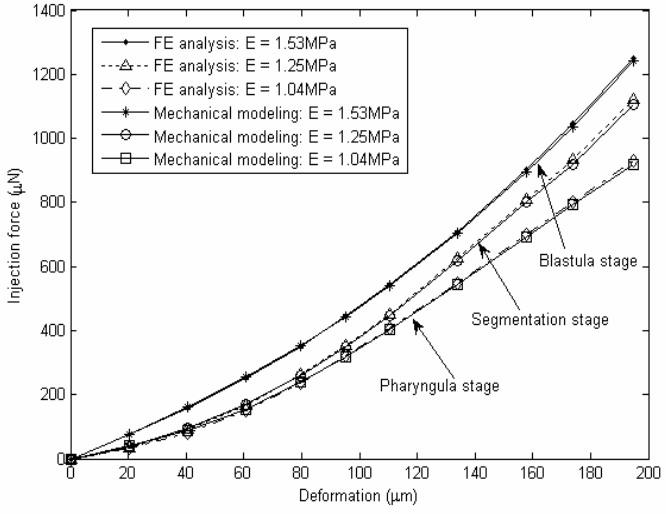

Fig. 7 Comparisons of FE analysis results and modeling results.

Besides the FE analysis, microrobotic cell injection experiments were performed to verify the mechanical model, and further for property characterization. The comparisons between the experimental and modeling results are shown in

Fig.8. It can be seen that through the property identification procedure the results obtained from the mechanical model agree well with the experiments at different developmental stages of zebrafish embryos, which also testifies that the mechanical model is applicable in modeling the deformation behavior of biological cells during microinjection.

The values of the quantitative measure δ are listed in Table I. It can be seen that the fitness between the experiments and the mechanical model is acceptable, especially at the blastula stage. When δ is minimized, the most appropriate value of the mechanical property is identified. The estimated elastic moduli of zebrafish embryos at three developmental stages are shown in Table II, specifically 1.5300 ± 0.0086 *MPa* at the blastula stage, 1.2499 ± 0.0180 *MPa* at the segmentation stage, and 1.0397 ± 0.0101*MPa* at the pharyngula stage, respectively. The values of the elastic moduli decrease distinctly from the blastula stage to pharyngula stage, which indicates the membrane softening of zebrafish embryos. Since 20 embryos at each developmental stage are tested, the standard deviations of the estimated elastic moduli are also given. As shown in Table II, the results suggest that the difference of the mechanical property is trivial among these injected embryos.

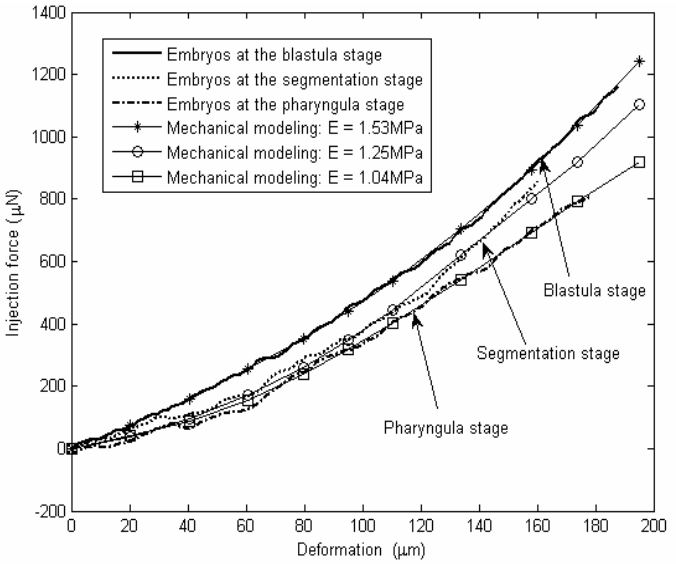

Fig. 8 Comparisons of the experimental results and modeling results

TABLE I
THE VALUE OF δ FOR ZEBRAFISH EMBRYOS

Stage	Blastula	Segmentation	Pharyngula
δ	8.4049e-4	0.0288	0.0336

TABLE II
CALCULATED ELASTIC MODULI FOR ZEBRAFISH EMBRYOS

Stage	Blastula	Segmentation	Pharyngula
Elastic modulus	1.5300	1.2499	1.0397
SD	0.0086	0.0180	0.0101

SD denotes the standard deviation of the calculated elastic modulus. Units for both of the quantities are *MPa*.

In conclusion, our developed model has been successfully verified by finite element analysis and microinjection experiments. It is demonstrated that our mechanical model can be used to model the mechanical responses of biological cells in microrobotic cell injection. Through the identification procedure, the elastic moduli of zebrafish embryos are obtained, which shows that microrobotic cell injection technology in combination with our mechanical model can be utilized to characterize the mechanical properties of biological cells.

Microinjection-based property characterization exhibits the following advantages. First, the cost of a cell injection system is low, and some commercial microinjection systems are now available. Second, since the microrobotic cell injection systems are semi-automatic or fully-automatic, it is easy to implement the injection operation, which ensures reliable measurements with high repeatability and high throughput.

IV. Conclusions

In this paper, to endow microrobotic cell injection system with the function of mechanical property characterization, a mechanical model is developed to model the deformation behavior of biological cells in microinjection. Finite element analysis and microrobotic cell injection experiments are conducted to verify this model. It is shown that the results obtained from the mechanical model agree well with that obtained from finite element analysis and the experiments, which demonstrates that microrobotic cell injection technology assisted by our mechanical model can be used to estimate the mechanical property of biological cells.

Acknowledgment

The authors would like to thank Dr. S. H. Cheng of the Department of Biology and Chemistry in City University of Hong Kong for cell collection and microinjector preparation.

References

[1] Y. Sun and B. J. Nelson, "Microrobotic cell injection," Proc. IEEE Int. Conf. on Robotics and Automation, pp. 620-625, 2001.

[2] Z. Lu, Peter C. Y. Chen, J. Nam, R. Ge, and W. Lin, "A micromanipulation system with dynamic force-feedback for automatic batch microinjection," J. Micromech. Mciroeng. vol. 17, pp. 314-321, 2007.

[3] L. Mattos, E. Grant, and R. Thresher, "Semi-automated blastocyst microinjection," Proc. IEEE Int. Conf. on Robotics and Automation, pp. 1780-1785, 2006.

[4] H. Huang, D. Sun, J. K. Mills, and S. H. Cheng, "Integrated vision and force control in suspended cell injection system: Towards automatic batch biomanipulation," Proc. IEEE Int. Conf. on Robotics and Automation, Pasadena, CA, USA, pp. 3413-3419, May 2008.

[5] E. M. Darling, S. Zauscher, J. A. Block, and F. Guilak, "A thin-layer model for viscoelastic, stress-relaxation testing of cells using atomic force microscopy: do cell properties reflect metastatic potential," Biophys. J., vol. 92, pp. 1784-1791, 2007.

[6] E. C. Faria, N. Ma, E. Gazi, P. Gardner, M. Brown, N. W. Clarke, and R.D. Snook, "Measurement of elastic properties of prostate cancer cells using AFM," Analyst, vol. 133, pp. 1498-1500, 2008.

[7] M. Lekka, P. Lardler, D. Gil, J. Lekki, Z. Stachura, and A. Z. Hrynkiewicz, "Elasticity of normal and cancerous human bladder cells studies by scanning force microscopy," Euro. Biophys. J., vol. 28, pp. 312-316, 1999.

[8] J. Guck, S. Schinkinger, B. Lincoln, F. Wottawah, S. Ebert, M. Romeyke, D. Lenz, H. M. Erickson, R. Ananthakrishnan, D. Mitchell, J. Kas, S. Ulvick, and C. Bilby, "Optical deformability as an inherent cell marker for testing malignant transformation and metastatic competence," Biophys. J., vol. 88, pp. 3689-3698, 2005.

[9] S. E. Cross, Y. S. Jin, J. Y. Rao, and J. K. Gimzewski, "Nanomechanical analysis of cells from cancer patients," Nature Nanotechnology, vol. 2, pp. 780-783, 2007.

[10] S. Suresh, "Elastic clues in cancer detection," Nature Nanotechnology, vol. 2, pp. 748-749, 2007.

[11] S. Park, D. Koch, R. Cardenas, J. Kas, and C. K. Shih, "Cell motility and local viscoelasticity of fibroblasts," Biophys. J., vol. 89, pp. 4330-4342, 2005.

[12] F. K. Glenister, R. L. Coppel, A. F. Cowman, N. Mohands, and B. M. Cooke, "Contribution of parasite proteins to altered mechanical properties of malaria-infected red blood cells," Blood, vol. 99, pp. 1060-1063, 2002.

[13] N. Kol, M. Gladnikoff, D. Barlam, R. Z. Shneck, A. Rein, and I. Rousso, "Mechanical properties of murine leukemia virus particles: effect of maturation," Biophys. J., vol. 91, pp. 767-774, 2006.

[14] E. A. Evans and R. M. Hochmuth, "Membrane viscoelasticity," Biophys. J., vol. 16, pp. 1-11, 1976.

[15] K. A. Ward, W. I. Li, S. Zimmer, and T. Davis, "Viscoelastic properties of transformed cells: role in tumor cell progression and metastasis formation," Biorheology, vol. 28, pp. 301-313,1991.

[16] E. K. Dimitriadis, F. Horkay, J. Maresca, B. Kachar, and R. S. Chadwick, "Determination of elastic moduli of thin layers of soft material using the atomic force microscope;" Biophys. J., vol. 82, pp. 2798–2810, 2002.

[17] D. Navajas, "Microrheology of human lung epithelial cells measured by atomic force microscopy," Biophys. J., vol. 84, pp. 2071–2079, 2003.

[18] Q. S. Li, G. Y. H. Lee, C. N. Ong, and C. T. Lim, "AFM indentation study of breast cancer cells," Biochem. Biophys. Res. Comm., vol. 374, pp. 609-613, 2008.

[19] N. O. Petersen, W. B. McConnaughey, and E. L. Elson, "Dependence of locally measured cellular deformability on position on the cell, temperature, and cytochalasin B," Proc. Natl. Acad. Sci. USA, vol. 79, pp. 5327–5331, 1982.

[20] B. Daily and E. L. Elson, "Cell poking: determination of the elastic area compressibility modulus of the erythrocyte membrane," Biophys. J., vol. 45, pp. 671-682, 1984.

[21] O. Thoumine and A. Ott, "Time scale dependent viscoelastic and contractile regimes in fibroblasts probed by microplate manipulation," J. Cell Sci., vol. 110, pp. 2109-2116, 1997.

[22] M. Beil, A. Micoulet, G. V. Wichert, S. Paschke1, P. Walther, M. B. Omary, P. P. V. Veldhoven, U. Gern1, E. Wolff-Hieber, J. Eggermann, J. Waltenberger, G. Adler1, J. Spatz, and T. Seufferlein, "Sphingosylphosphorylcholine regulates keratin network architecture and visco-elastic properties of human cancer cells," Nature Cell Biology, vol. 5, pp. 803-811, 2003.

[23] A. R. Bausch, W. Moller, and E. Sackmann, "Measurement of local viscoelasticity and forces in living cells by magnetic tweezers," Biophys. J., vol. 76, pp. 573–579, 1999.

[24] S. Henon, G. Lenormand, A. Richert, and F. Gallet, "A new determination of the shear modulus of the human erythrocyte membrane using optical tweezers," Biophys. J., vol. 76, pp. 1145–1151, 1999.

[25] J. Sleep, D. Wislon, R. Simmons, and W. Gratzer, "Elasticity of the red cell membrane and its relation to hemolytic disorders: an optical tweezers study," Biophys. J., vol. 77, pp. 3085–3095, 1999.

[26] A. D. Mehta, M. Rief, J. A. Spudich, D. A. Smith, and R. M. Simmons, "Single-molecule biomechanics with optical methods," Science, vol. 283, pp. 1689-1695, 1999.

[27] J. Guck, R. Ananthakrishnan, H. Mahmood, T. J. Moon, C. C. Cunningham, and J. Kas, "The optical stretcher: a novel laser tool to micromanipulate cells," Biophys. J., vol. 81, pp. 767–784, 2001.

[28] J. Kuncova and P. Kallio, "Challenges in capillary pressure microinjection," Proc. IEEE Int. Conf. EMBS, pp. 4998-5001, 2004.

[29] Iritani A., "Micromanipulation of gametes for in vitro assisted fertilization," Mol. Reprod. Dev., vol. 28, pp. 199-207, 1991.

[30] K. K. Tan, D. C. Ng, and Y. Xie, "Optical intra-cytoplasmic sperm injection with a piezo micromanipulator," The 4th world congress on Intelligent control and Automation, pp. 1120-1123, 2002.

[31] W. H. Wang, X. Y. Liu, D. Gelinas, B. Ciruna, and Y. Sun, "A fully automated robotic system for microinjection of zebrafish embryos," PLOS ONE, vol. 2, no. 9, pp. 862, 2007

[32] X. J. Zhang, C-C Chen, R. W. Bernstein, S. Zappe, M. P. Scott, and O. Solgaard, "Microoptical characterization and modeling of positioning forces on Drosophila embryos self-assembled in two-dimensional arrays," J. MicroElectroMechanical Systems, vol. 14, no. 5, pp. 1187-1197, 2005

[33] X. D. Li, G. Zong, and S. Bi, "Development of global vision system for biological automatic micromanipulation system," Proc. IEEE Int. Conf. on Robotics and Automation, vol. 1, pp. 127-132, 2001.

[34] Y. Xie, D. Sun, C. Liu, S. H. Cheng, and Y. H. Liu, "A force control based cell injection approach in a bio-robotics system," Proc. IEEE Int. Conf. on Robotics and Automation, Kobe, Japan, pp. 3143-3148, May 2009.

[35] Y. Sun, K. T. Wan, K. P. Roberts, J. C. Bischof, and B. J. Nelson, "Mechanical property characterization of mouse zona pellucida," IEEE Trans. on NanoBioScience, vol. 2, pp. 279-286, 2003.

[36] H. B. Huang, D. Sun, J. K. Mills, and W. J. Li, "Visual-based impedance control of out-of-plane cell injection systems," IEEE Trans. on Automation Science and Engineering, vol. 6, no. 3, pp. 565-571, July 2009.

[37] H. B. Huang, D. Sun, J. K. Mills, and W. J. Li, "Visual-based impedance force control of three-dimensional cell injection system," Proc. IEEE Int. Conf. on Robotics and Automation, pp. 4196-4201, 2007.

[38] Y.T. Shen, Wejinya, U.C., N. Xi, and C. A. Pomeroy, "Force measurement and mechanical characterization of living Drosophila embryos for human medical study," Proceedings of the Institutions of Mechanical Engineers, Part H: Journal of Engineering in Medicine, vol. 221, no. 2, pp. 99-112, January 2007

[39] Wejinya, U.C., Y.T. Shen, and N. Xi, "In situ micro-force sensing and quantitative elasticity evaluation of living Drosophila embryos at different stages" Proc. IEEE/ASME Int. Conf. on Advanced Intelligent Mechatronics, Xi'an, China, pp. 498-503, July 2008.

[40] H. B. Huang, D. Sun, J. K. Mills, and S. H. Cheng, "Robotic cell injection system with vision and force control: Towards automatic batch biomanipulation," IEEE Trans. on Robotics, vol. 25, no. 3, pp. 727-737, June 2009.

[41] Y. H. Tan, D. Sun, W. H. Huang, and S. H. Cheng, "Mechanical modeling of biological cells in microinjection," IEEE Trans. on NanoBioScience, vol. 7, no. 4, pp. 257-266, Dec. 2008.

[42] L. D. Landau and E. M. Lifshitz, "Theory of elasticity," Pergamon, New York, 1986.

[43] Z. Zhang, M. A. Ferenczi, and C. R. Thomas, "A micromanipulation technique with a theoretical cell model for determining mechanical properties of single mammalian cells," Chem. Eng. Sci., vol. 47, pp. 1347-1354, 1992.

[44] T. J. Lardner and P. Pujara, "Compression of spherical cells," in Mechanics Today, vol. 5, pp. 161-176, 1980.

[45] W. W. Feng and W. H. Yang, "On the contact problem of an inflated spherical nonlinear membrane," J. Appl. Mech., vol. 40, pp. 209-214, 1973.

[46] L. Y. Cheng, "Deformation analyses in cell and developmental biology Part I-Formal methodology," J. Biomech. Eng., vol.109, pp.10-17, 1987.

[47] K. K. Liu, D. R. Williams, and B. J. Briscoe, "Compressive deformation of a single microcapsule," Phys. Rev. E, vol. 54, no. 6, pp. 6673-6680, 1996.

[48] Laurene Fausett, "Numerical methods: algorithms and applications," Prentice Hall, 2003.

[49] http://www.dynacitytech.com.

[50] Monte Westerfield, "The zebrafish book: a guide for the laboratory use of zebrafish (Danio rerio)," The third edition, 1995.

[51] C. E. Schmidt, T. Chen, and D. A. Lauffenburger, "Simulation of integrin-cytoskeletal interactions in migrating fibroblasts," Biophys. J., vol. 67, pp. 461-474, 1994.